Photon Netw Commun (2016) 32:179–187
DOI 10.1007/s11107-016-0617-4

A Q-band radio-over-fiber system for distribution of uncompressed high-definition video signals

Zhenzhou Tang[1] · Shilong Pan[1]

Received: 22 November 2015 / Accepted: 15 February 2016 / Published online: 10 March 2016

Abstract A Q-band radio-over-fiber (RoF) system for transmission of uncompressed high-definition (HD) video signals is proposed and demonstrated. Three key photonic technologies are employed, i.e., the dispersion compensation based on a polarization modulator and a polarizer in the transmitter, the RF carrier extraction based on injection-locked optoelectronic oscillator and the frequency downconversion based on cascaded external modulations in the receiver. A proof-of-concept experiment is carried out. Results show that the proposed system supports 20-km wired and 0.5-m wireless distribution of uncompressed HD video signal. The cooperation of two antennas is also demonstrated, which provides a preliminary demonstration of intelligent RoF system.

Keywords Radio over fiber · Optoelectronic oscillator · Carrier extraction · Dispersion compensation · Microwave photonics

1 Introduction

According to the global mobile data traffic forecast by Cisco Inc. in February 2015 [1], the wireless video services have been one of the major bandwidth consumers to the global mobile data traffic, which contributes more than 50 % of the global mobile data traffic by 2014, and will grow to three-fourths by 2019. Moreover, with the continuous pursuit of quality of viewing experience for users, the data rate of the video service has increased substantially with the improvement of the video resolution in recent years. Taking the ultra-high-definition TV (UHDTV) as an example, it requires at least 24 Gb/s data rate, which is 36 times higher than that of the 720p high-definition (HD) TV. However, up to date, the highest transmission data rate based on commercial 4G wireless communication system is only about 100 Mbps, which is far from enough for wireless transmission of uncompressed HD videos.

One effective scheme for the high-speed wireless communication is to increase the carrier frequency to the millimeter-wave band, which can provide more spectrum resource. For instance, the 60-GHz band gigabit-class wireless communication standards, IEEE 802.15.3c [2], ECMA-387 [3] and IEEE 802.11ad [4], have already been established in 2009, 2010 and 2012, respectively, and the potential of using THz wave for wireless communication was also discussed recently [5]. As the increasing in the carrier frequency, the high air-link loss becomes a critical problem, which would restrict the transmission distance of the wireless system. To increase the area of coverage and to offer the availability of undisrupted service across the millimeter-wave network and other conventional networks, radio-over-fiber (RoF) technology has been proposed [6–8]. In the RoF system, the optical RF signals are generated in the center office (CO) and distributed to the remote antenna units (RAUs) via low-loss optical fibers. Since this architecture allows all the complex and expensive components to be shifted to the CO, it enables simple RAU design, centralized resource allocation and multi-channel operation with a unified platform. Previously, lots of RoF systems for distribution of wireless services with high data rate, most of which are working at 60 GHz or higher-frequency band, have been reported in the literature [9–14]. Since the state of the art in the electro-optic modulator cannot cover the 60-GHz band or above, a key problem associated with the 60-GHz or higher-frequency band RoF

✉ Shilong Pan
pans@nuaa.edu.cn

1 Key Laboratory of Radar Imaging and Microwave Photonics, Ministry of Education, Nanjing University of Aeronautics and Astronautics, Nanjing 210016, China

system is the electro-optical conversion. To solve this problem, sophisticated RoF transmitter has to be applied.

In this paper, we propose a Q-band RoF system for the distribution of uncompressed HD video signal. Q-band (40.5–47 GHz) is suggested for short-range communication in China and a protocol named IEEE 802.11aj will be released in 2016 [15]. The huge unlicensed bandwidth (5.9 GHz) coupled with moderate transmit power and rapid advances in integrated circuit (IC) technologies makes Q-band a promising candidate for the high data rate wireless communication. Besides, as compared with the 60-GHz band RoF systems, no sophisticated transmitters are required in the Q-band RoF systems, since the commercially available electro-optic modulators can easily cover this frequency band. Three key technologies are employed in the proposed RoF system: (1) to eliminate the power fading introduced by the fiber dispersion, a polarization modulator (PolM) and a polarizer are used in the transmitter; (2) in the receiver, an injection-locked optoelectronic oscillator (OEO) is applied to extract the electrical carrier from the incoming Q-band RF signal; (3) with the extracted carrier, wideband photonic microwave mixing is employed to downconvert the Q-band RF signal to the baseband. The proposed system is demonstrated at laboratory environment. An uncompressed HD video signal is successfully distributed through a 20-km wired and 0.5-m wireless link. In addition, the cooperation of the antennas is also investigated, which provides a preliminary demonstration for intelligent RoF system.

2 Principle

2.1 System architecture

The schematic diagram of the proposed Q-band RoF system is depicted in Fig. 1. In the CO, a baseband uncompressed HD video signal output from a HD video player is upconverted to the Q-band by mixing with a 40-GHz LO at an electrical mixer. The upconverted RF signal is then modulated to a lightwave from a laser diode (LD, LD1) via a PolM. The optical microwave signal is sent to a polarization controller (PC) and a polarization beam splitter (PBS) to perform polarization modulation to intensity modulation conversion. After being amplified by an erbium-doped fiber amplifier (EDFA), the optical signal is transmitted to the RAU through a length of single-mode fiber (SMF). In the RAU, the optical microwave signal is converted to an electrical signal by a photodector (PD1). The electrical signal is then amplified by an electrical amplifier (EA, EA1) and emitted to the free space through a horn antenna.

In the receiver, the signal is collected by another horn antenna. The received signal is amplified by a second EA (EA2) and converted back to the optical domain at a Mach–

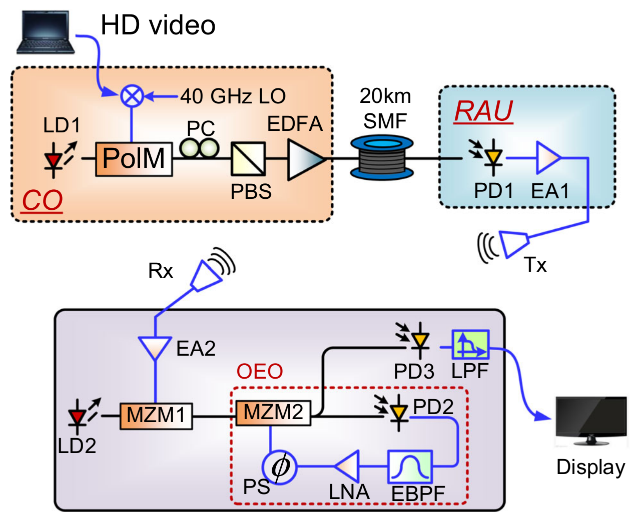

Fig. 1 Schematic diagram of the proposed Q-band RoF system. *LD* laser diode, *PolM* polarization modulator, *PC* polarization controller, *PBS* polarization beam splitter, *EDFA* erbium-doped fiber amplifier, *SMF* single-mode fiber, *PD* photodetector, *EA* electrical amplifier, *LNA* low-noise amplifier, *MZM* Mach–Zehnder modulator, *EBPF* electrical bandpass filter, *PS* phase shifter, *LPF* low-pass filter

Zehnder modulator (MZM, MZM1). The optical microwave signal from MZM1 is sent to an OEO. The OEO is consisted of another MZM (MZM2), a PD (PD2), a high-Q electrical bandpass filter (EBPF), a low-noise amplifier (LNA) and a phase shifter (PS). The output signal of the OEO is launched to a PD (PD3). A low-pass filter (LPF) is used to select the baseband HD video signal. The baseband HD video signal is finally sent to a HD display.

2.2 Dispersion compensation

It is well known that for the conventional intensity modulation-direct detection (IM/DD) RoF link based on double sideband (DSB) modulation, the fiber dispersion will introduce a frequency response given by $H(f_{\mathrm{m}}) \propto \cos^2(\pi D L \lambda^2 f_{\mathrm{m}}^2/c)$, where D and L are the dispersion parameter and the length of the fiber, λ is the wavelength of the carrier, f_{m} is the RF frequency and c is the velocity of the light in vacuum [16]. If the fiber dispersion was not compensated, it would result in periodic power fading, which significantly degrades the performance of the link. To solve this problem, one can employ the optical single sideband (OSSB) modulation [17,18] or the method based on optical phase conjugation [19], carrier phase-shifted DSB modulation [20] or pre-compensation in the electrical domain [21]. But these methods are hard to achieve wideband and wavelength tunable operation. Moreover, additional electrical devices (e.g., 90° hybrid coupler in [17]) or optical components (e.g., fiber Bragg grating in [18]) are usually needed in the transmitter, which would introduce the complexity of the transmitter.

In the proposed system, the dispersion is compensated by the PolM together with a PC and a PBS in the transmitter, in which the PC and PBS function as a polarizer [22]. To simplify the analysis, we assume that the signal applied to the PolM is a single-tone RF signal with an angular frequency of ω_{m}. At the output of PolM, two phase-modulated optical waves along the two principal axes are generated [23]

$$\begin{bmatrix} E_x \\ E_y \end{bmatrix} = \frac{\sqrt{2}}{2}\begin{bmatrix} \exp(j\omega_{c1}t + j\beta\cos\omega_{\mathrm{m}}t) \\ \exp(j\omega_{c1}t - j\beta\cos\omega_{\mathrm{m}}t) \end{bmatrix} \tag{1}$$

where ω_{c1} is the angular frequency of the optical carrier generated by LD1, β is the modulation index and E_x and E_y are then combined by the PBS, whose principal axis is oriented at an angular of α to one principal axis of the PolM. The output signal is given by

$$\begin{aligned} E_1 &= \cos\alpha E_x \exp(j\phi_0) + \sin\alpha E_y \\ &\propto \exp(j\omega_{c1}t)\left[\cos\alpha\cdot\exp(j\beta\cos\omega_{\mathrm{m}}t + j\phi_0) \right.\\ &\quad \left. + \sin\alpha\cdot\exp(-j\beta\cos\omega_{\mathrm{m}}t)\right] \\ &= \exp(j\omega_{c1}t)\cdot[\cos\alpha\cdot\exp\left(j\frac{\phi_0}{2}\right)\cdot \\ &\quad \times \underbrace{\cos\left(\beta\cos\omega_{\mathrm{m}}t + \frac{\phi_0}{2}\right)}_{\text{amplitude modulation}} \\ &\quad + (\sin\alpha - \cos\alpha)\cdot\underbrace{\exp(-j\beta\cos\omega_{\mathrm{m}}t)}_{\text{phase modulation}}] \end{aligned} \tag{2}$$

where ϕ_0 is the phase difference between E_x and E_y which can be adjusted by tuning the DC bias applied to the PolM. As can be seen from (2), PolM can simultaneously support both amplitude modulation and phase modulation, and the ratio of the two modulations, i.e., α, can be adjusted by tuning the PC inserted between the PolM and the PBS. If the optical signal in (2) is sent to the SMF, the signal after transmission is written by

$$\begin{aligned} E_2 &= \exp(j\omega_{c1}t)\left\{\left[J_0\cdot\exp(j\phi_0)\cos\alpha + \sin\alpha\right)\exp(j\theta_0)\right] \\ &\quad + \left[jJ_1\cdot(\exp(j\phi_0)\cos\alpha - \sin\alpha)\exp(j(-\omega_{\mathrm{m}}t + \theta_{-1}))\right] \\ &\quad + \left[jJ_1\cdot(\exp(j\phi_0)\cos\alpha - \sin\alpha)\exp(j(\omega_{\mathrm{m}}t + \theta_{+1}))\right]\right\} \end{aligned} \tag{3}$$

where J_n is the nth-order Bessel function of the first kind. In (3), higher-order (≥ 2) terms are ignored due to small-signal modulation $\theta_0 = z\beta(\omega_{c1})$, $\theta_{+1} = z\beta(\omega_{c1}) + \tau_0\omega_{\mathrm{m}} + 1/2D_\omega\omega_{\mathrm{m}}^2$, and $\theta_{-1} = z\beta(\omega_{c1}) - \tau_0\omega_{\mathrm{m}} + 1/2D_\omega\omega_{\mathrm{m}}^2$ are the dispersion-induced phase shifts to the optical carrier and the upper and lower sidebands, respectively, where z is the traveling distance, $\beta(\omega_{c1})$ is the propagation constant at ω_{c1}, $\tau_0 = z\beta'(\omega_{c1})$ and $D_\omega = z\beta''(\omega_{c1})$. When the signal is launched to PD1, and let $\phi_0 = \pi/2$, we can obtain the AC term of the detected signal

$$i_{\mathrm{AC}} = \left|E'(t)\right|^2 \propto \sin\left(2\alpha + \frac{1}{2}D_\omega\omega_{\mathrm{m}}^2\right)\cos[\omega_{\mathrm{m}}(t - \tau_0)] \tag{4}$$

As can be seen, the power of the generated electrical signal has a coefficient given by $\eta = \sin(2\alpha + 1/2D_\omega\omega_{\mathrm{m}}^2)$. If α changes, the coefficient will also change. When $2\alpha + 1/2D_\omega\omega_{\mathrm{m}}^2 = (2k+1)\pi/2, k = 0, \pm1, \pm2\ldots$, the signal at ω_{m} will have the maximum transmittance, which means the power fading around the carrier frequency of ω_{m} is compensated. Therefore, in the proposed RoF system, based on the same principle, the fiber-introduced dispersion around the RF carrier can be easily compensated by properly setting the PC in the transmitter.

2.3 Electrical carrier extraction

In the receiver, the uncompressed HD video signal should be downconverted from the Q-band back to the baseband for processing and display. To do so, an LO signal is usually employed to mix with the received RF signal. To ensure the conversion performance, the frequency and phase of the used LO should be identical to that of the carrier in the received RF signal. Conventionally, the LO signal is produced by an external microwave source, so each receiver should be equipped with a LO source, and complex frequency and phase synchronization should also be applied. To reduce the complexity of the receiver, extracting the carrier from the RF signal without using the external LO signals is preferred.

OEO is an effective way to perform the electrical carrier extraction. An OEO is an optoelectronic feedback loop, which consists of an intensity modulator, an optical fiber, a PD, an electrical amplifier and a high-Q EBPF [24]. If a continuous-wave (CW) light without any data is sent to the modulator, the OEO will be working at free-running mode, in which it oscillates at one of its eigenmodes determined by the center frequency of the EBPF. However, if the optical signal applied to the OEO loop contains an electrical carrier with a frequency near the free-running oscillating frequency, the OEO will be injection-locked [25]. Under the injection-locking condition, the oscillating signal of the OEO would be frequency- and phase-locked to the electrical carrier, while other frequency components are suppressed.

In the proposed system, the RF signal collected by the antenna is modulated on the optical carrier generated by LD2 at MZM1 and sent to the OEO. The center frequency of the EBPF in the OEO is chosen to be near the electrical carrier frequency of the received RF signal, so the OEO would be injection-locked, i.e., an electrical signal with a frequency that is identical to the electrical carrier of the received RF signal is oscillated in the OEO loop.

2.4 Frequency downconversion

As mentioned above, the received Q-band RF signal should be mixed with an LO signal to downconvert the HD video signal back to the baseband. Since a high-quality LO signal is obtained by the OEO in the optical domain, performing the frequency downconversion based on the photonic technology becomes preferable, since no additional optical-to-electrical or optical-to-electrical conversion is needed. In addition, compared to the conventional electrical mixer, the photonic-based mixer has the advantages in terms of ultra-high isolation and immunity to electromagnetic interference.

A lot of photonic microwave downconversion methods have been reported [26–29]. In our proposed system, two cascaded intensity modulators (MZM1 and MZM2 in Fig. 1) are used to realize the photonic frequency downconversion [26]. Since the OEO loop is oscillated at ω_m, the architecture of the receiver is shown in Fig. 2. When the received RF signal is modulated onto the optical carrier at MZM1, two sidebands with the frequency spacing of the RF carrier ω_m would be generated around the optical carrier. Figure 2a, b show the schematic optical spectra of the optical carrier and the modulated signal, respectively. Then, the optical microwave signal in Fig. 2b is sent to MZM2, which is driven by the electrical carrier extracted by the OEO loop. Due to the electro-optical modulation effect, the incoming optical microwave signal would be remodulated, which generates additional sidebands with frequency spacing of ω_m around each of the frequency components. Figure 2c shows the optical spectrum after remodulation. When the output signal from MZM2 is launched to PD3, due to the frequency beating between the RF sidebands and the LO sidebands, a baseband HD video data would be obtained if an LPF is followed after PD3, which can be seen from the illustration shown in Fig. 2d.

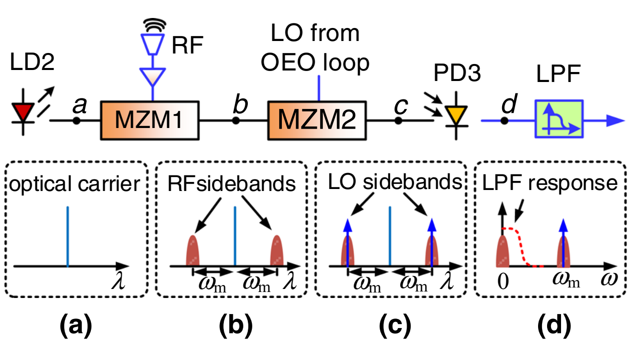

Fig. 2 Principle of the frequency downconversion in the receiver of the proposed RoF system. *a–c* The optical spectra of the signals at points *a–c* and (*d*) the electrical spectrum of the signal at the output of PD3

3 Experiment and results

An experiment based on the configuration shown in Fig. 1 is carried out. At the transmitter, a 1.5-Gb/s uncompressed HD video outputs from a HD video player is mixed with a 40-GHz LO (Agilent E8257D) at an electrical mixer (Marki M9-0444) and converted into an optical microwave signal by modulating a CW lightwave at the PolM (Versawave Technologies). The CW lightwave is generated by LD1 (Teraxion PS-NLL-1550.52-80-04). The PolM has a bandwidth of 40 GHz and a half voltage of 3.5 V. The optical microwave signal travels through a PC and a PBS to perform polarization modulation to intensity modulation conversion. After being amplified by an EDFA (Amonics AEDFA-35-B-FA), the optical signal is sent to the RAU through a 20-km SMF. At the RAU, the optical microwave signal is converted back to an electrical signal at PD1 (u2t 2120R) with a bandwidth of 50 GHz and a responsivity of 0.65 A/W. The electrical signal is then amplified by EA1 (SHF 806E) with a gain of 26 dB within the frequency range of 40 kHz–38 GHz, and emitted to the free space through a horn antenna.

In the receiver, LD2 generates a CW lightwave and sent to MZM1 (Fujitsu FTM7938EZ) with a bandwidth of 40 GHz and a half-wave voltage of 2.8 V. The RF signal, collected by another horn antenna, is amplified by EA2 (SHF 806E) and sent to MZM1. The optical microwave signal is injected into the OEO-based frequency downconversion module. In the OEO, the incoming optical signal is went through MZM2 (Fujitsu FTM7938) and split into two branches. The lower branch is feedback to the RF port of MZM2 through PD2 (u2t 2120R) with a bandwidth of 50 GHz and responsivity of 0.65 A/W, an EBPF with a center frequency of 40 GHz and a bandwidth of 20 MHz, a 40-GHz LNA with a gain of 40 dB and a 40-GHz phase shifter. The upper branch is sent to PD3 with a bandwidth of 10 GHz and a responsivity of 0.85 A/W. An LPF with a cut frequency of 2.2 GHz is followed to select the baseband HD video signal. The selected HD video is sent to a HD video display.

The electrical spectra are measured by an electrical spectrum analyzer (Agilent E4447A), and the eye diagrams are observed by a sampling oscilloscope (Agilent 86100A). In addition, an optical spectrum analyzer (YOKOGAWA AQ6370C) is used to measure the optical spectra.

To evaluate the performance of the proposed Q-band RoF link, a 2-Gbps pseudo-random binary sequence (PRBS) signal generated by a pulse pattern generator (Anritsu MP1763C) is employed as the input baseband signal. Figure 3a shows the electrical spectrum of the upconverted Q-band RF signal when the PRBS data are mixed with a 40-GHz LO. The zoom-in view of the spectrum within the frequency range of 37–43 GHz is shown in Fig. 3b. The Q-band RF signal is converted to an optical signal in the transmitter and sent to the RAU through the 20-km fiber

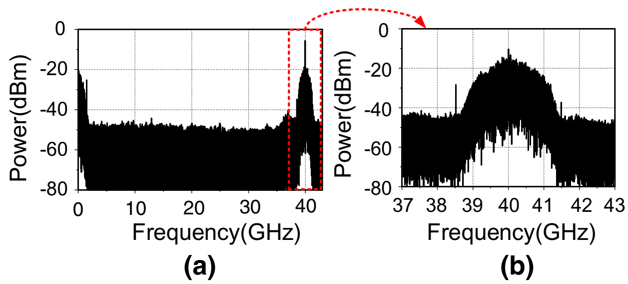

Fig. 3 (**a**) The electrical spectrum of the upconverted Q-band RF signal in the CO and (**b**) the zoom-in view of the spectrum within the frequency range of 37–43 GHz

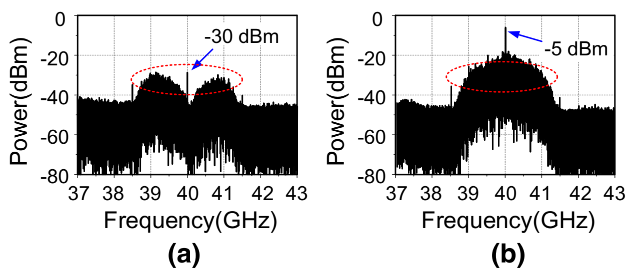

Fig. 4 The electrical spectra of the signal after SMF transmission (**a**) without and (**b**) with the dispersion compensation

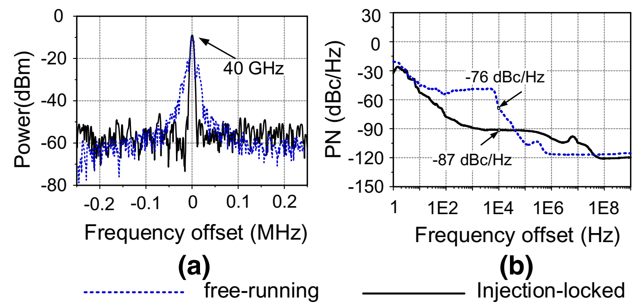

Fig. 5 (**a**) Electrical spectra and (**b**) phase noise of the oscillating signals when the OEO is working in the injection-locking mode (*solid line*) and free-running mode (*dashed line*)

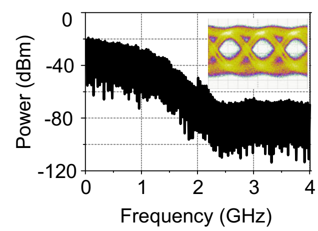

Fig. 6 The electrical spectrum of the downconverted PRBS signal in the receiver. Inset: the corresponding eye diagram

link. Figure 4a shows the electrical spectrum of the RF signal obtained by PD1 if the dispersion is not compensated. As can be seen, the power of the transmit signal is highly distorted because of the fiber dispersion. Compared with the spectrum shown in Fig. 3b, the power of the RF carrier is only −30 dBm, which is difficult for clock extraction in the receiver. Moreover, the video data close to the RF carrier are also suppressed, which would introduce considerable errors. However, according to the analysis in Sect. 2, when adjusting the PC placed before the PBS to make $2\alpha + 1/2D_{\omega}\omega_{\mathrm{m}}^2 = (2k+1)\pi/2$, the fiber dispersion can be effectively compensated. Figure 4b shows the electrical spectrum after dispersion compensation. As can be seen, the RF signal after fiber transmission is nearly unchanged, and a similar spectral profile can be observed. The power of the RF carrier is increased to −5 dBm. It should be noted that the original baseband data would not be emitted through the horn antenna, since the antenna has a bandwidth of 26.5–40 GHz.

In the receiver, when the RF signal is not applied to MZM1, the OEO loop will work in the free-running mode. The electrical spectrum and phase noise of the oscillating signal are shown as the dashed line in Fig. 5a, b respectively. As can be seen from Fig. 5a, since the EBPF has a center frequency of 40 GHz, a microwave signal around 40 GHz is generated. However, due to the environmental disturbance, a wide spectral linewidth can be observed, which means the stability of the generated signal is poor. The phase noise in Fig. 5b gives the same conclusion, which is only −76 dBc/Hz at the frequency offset of 10 kHz. When the received RF signal is applied to MZM1, the OEO would be injection-locked. As a result, the RF carrier will be extracted by the OEO. The electrical spectrum of the oscillating signal in the injection-locking mode is shown as the solid line in Fig. 5a, and the corresponding phase noise is shown in Fig. 5b. As can be seen, an exact 40-GHz microwave signal is generated in the OEO loop. The spectral linewidth is very narrow, and the phase noise of the injection-locked RF signal at 10 kHz offset is 87 dBc/Hz, 11-dB lower than that of the free-running signal. Both the electrical spectrum and phase noise show that a frequency- and phase-stable RF carrier is extracted by the OEO, which agrees well with the analysis in Sect. 2.

With the exacted high-stable 40-GHz RF carrier, photonic frequency downconversion is achieved at the output of PD3. Figure 6 shows the electrical spectrum of the baseband signal after the LPF. The eye diagram of the signal is also shown as the inset in Fig. 6. The eye is widely open, indicating that error-free transmission is achieved. The bit error rate (BER) performance for the transmission of the PRBS signal is also measured. The receiver sensitivity for the back-to-back (BTB) case is −6 dBm while that for 20-km SMF transmission is −5.5 dBm, giving a power penalty of 0.5 dB.

Then, the PRBS signal is replaced by a 1.5-Gb/s uncompressed HD video signal. The spectra of the downconverted video signal in the receiver and the original video signal in the transmitter are shown in Fig. 7a, b, respectively. Similar spectral profiles are observed after transmission through the proposed Q-band RoF system. Figure 8 shows the pho-

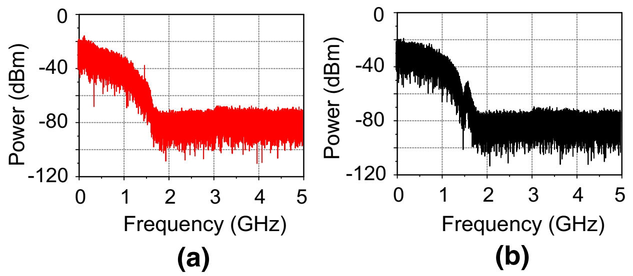

Fig. 7 The electrical spectra of the uncompressed HD video signal in the (**a**) receiver and (**b**) transmitter

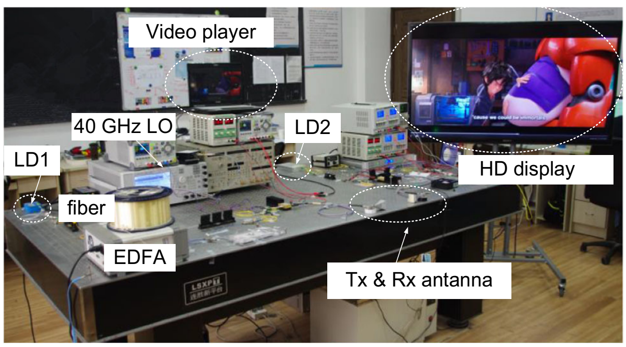

Fig. 8 The photograph of the video transmission system

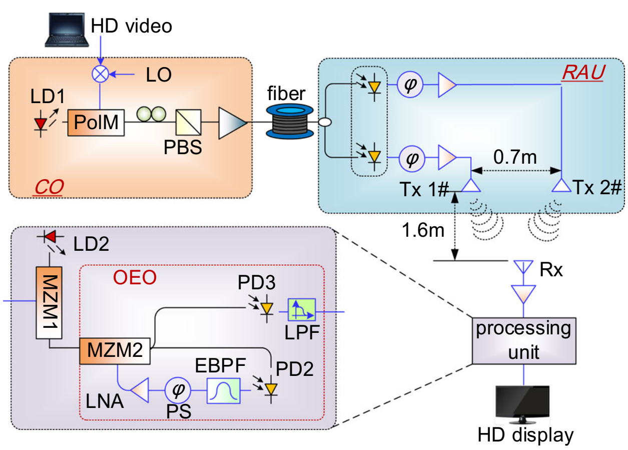

Fig. 9 Schematic diagram of the RoF system when two transmit antennas and one receive antenna are used

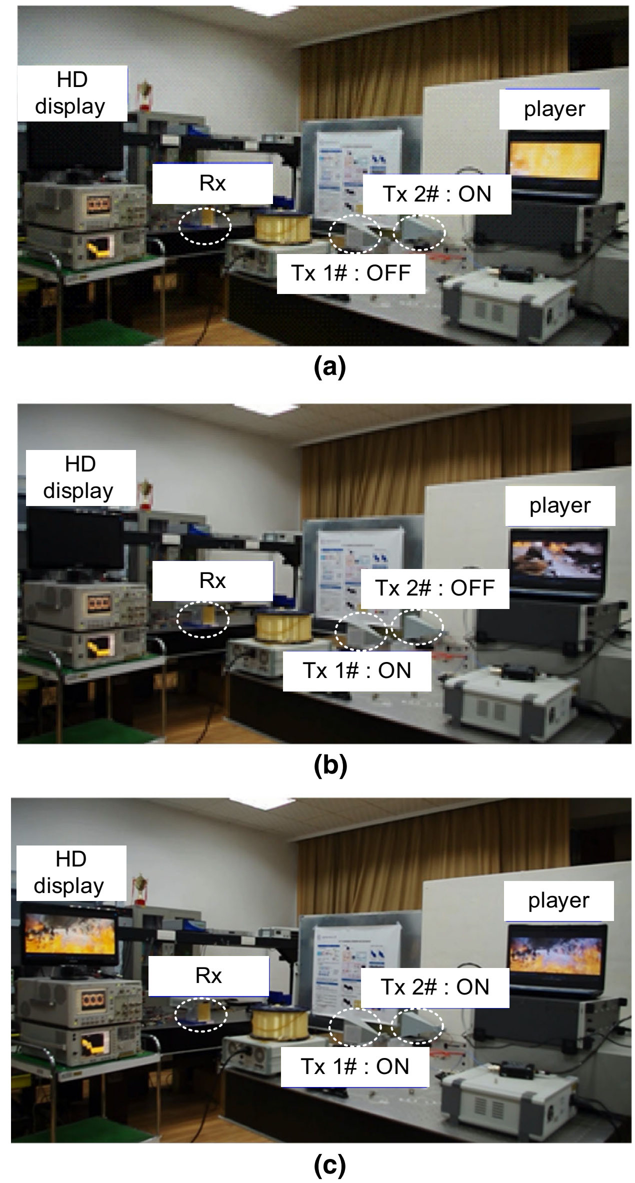

Fig. 10 Photographs of experimental system when (**a**) only Tx 2# works, (**b**) only Tx 1# works, and (**c**) both Tx 1# and Tx 2# work

tograph of the proposed RoF system. As can be seen, the real-time display of the video in the remote site is realized and the received video is well synchronized to the source in the transmitter. Thanks to the automatically track of the phase by the injection-locked OEO, the system is operated in the laboratory environment for more than half an hour without any interruption.

The aforementioned RoF system shows a basic demonstration for the high data rate video service distribution. However, for a practical system, a lot of RAUs would be connected to the CO. To offer wireless servers with higher quality, technologies such as remote spectral sensing, dynamic resource allocation and cooperation between RAUs, should be introduced. Therefore, the corporation of two antennas in the proposed system is investigated.

Considering that if the power of the signal emits from a single antenna is not strong enough to drive the receiver in the user end, multiple antennas can be controlled to provide the same service to a common user. Figure 9 shows the condition that two transmit antennas (Tx 1# and Tx 2#) are working together to send the same RF signal to a single receiver (Rx).

To demonstrate the corporation between Tx 1# and Tx 2#, we reduce the signal power emitting from a single antenna, so

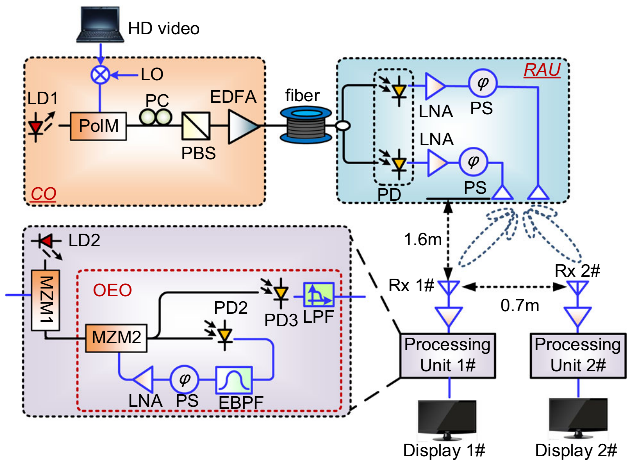

Fig. 11 Schematic diagram of the beamforming-based RoF system

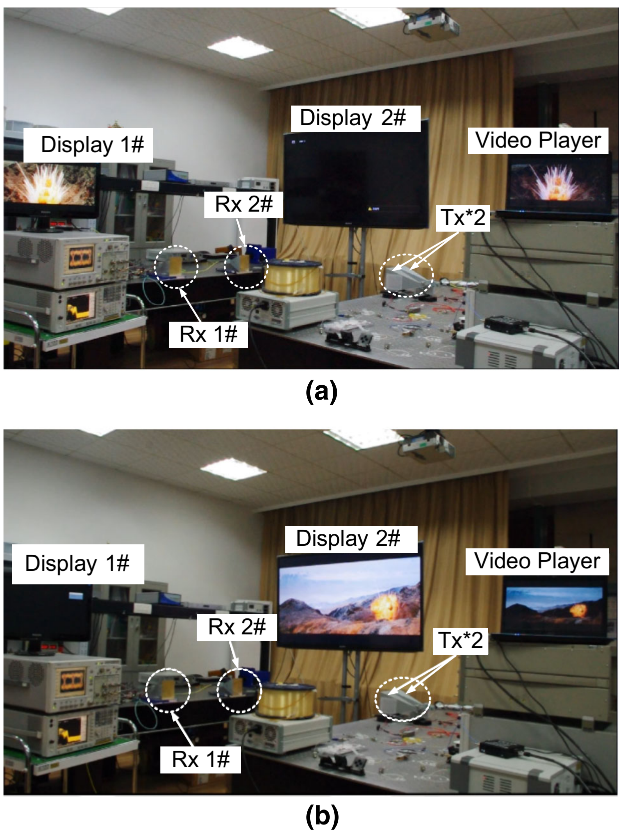

Fig. 12 Photographs of experimental system when the beam is pointed to (**a**) Rx 1# and (**b**) Rx 2#

that the received HD video signal is too small to be displayed on the display when only a single transmit antenna works. Figure 10a, b show the photographs of the system when only Tx 2# or Tx 1# works, in which the receive HD display cannot show the video. Then both Tx 1# and Tx 2# are enabled, and the received signal power would be increased. As can be seen from Fig. 10c, stable HD video appears in the receiving HD display.

Beamforming is another technique for the corporation of multiple antennas, in which the spacing of the antennas should be small enough to avoid grating lobes [30]. Beamforming can improve the capacity and robust of the wireless networks, and through electrically or optically control of the direction of the transmit beams, the co-channel and inter-channel interference can be dramatically reduced. Figure 11 shows the schematic diagram of the proposed beamforming-based RoF system. Two transmit antennas (Tx 1# and Tx 2#) and two receive antennas (Rx 1# and Rx 2#) are used.

By properly setting the phase shift of the each path in the RAU, the electrical beam would point to the desired receive antenna. Figure 12a shows the photograph of the system when the electrical beam is pointed to Rx 1#. As can be seen, only display 1# connected to Rx 1# works. On the other hand, when the phases are tuned to make the transmit beam point to Rx 2#, display 2# starts to work, as shown in Fig. 12b.

4 Conclusion

We have proposed a 40-GHz RoF system for the distribution of uncompressed HD video signal. Three key photonic technologies are employed and investigated, which are the fiber dispersion compensation based on a PolM in conjunction with a PC and a PBS, RF carrier extraction based an injection-locked 40-GHz OEO, and photonic microwave downconversion based on cascaded external modulations. An experiment is carried out at the laboratory environment. An uncompressed HD video signal is successfully distributed through a 20-km wired and 0.5-m wireless link. The cooperation between the antennas is also demonstrated in this paper. The proposed RoF system may find applications in the next-generation wireless communication systems.

Acknowledgments This work was supported in part by the National Basic Research Program of China (2012CB315705), the National Natural Science Foundation of China (61422108, 61527820) and the Fundamental Research Funds for the Central Universities.

References

[1] Cisco Inc., Cisco visual network index: global mobile data traffic forecast update, 2014–2019, 3 Feb (2015)
[2] IEEE STD 802.15.3C-2009. IEEE standard for information technology—local and metropolitan area networks—specific requirements—part 15.3: amendment 2: millimeter-wave-based alternative physical layer extension. 2009
[3] STANDARD ECMA-387. High Rate 60 GHz PHY, MAC and HDMI PALs, 2nd Edition. 2010
[4] IEEE STD 802.11AD-2012. IEEE standard for information technology—telecommunications and information exchange between systems—local and metropolitan area networks—specific requirements—part 11: wireless medium access control

(MAC) and physical layer (PHY) specifications—amendment 3: enhancements for very high throughput in the 60 GHz Band. 2012
[5] Song, H.J., Nagatsuma, T.: Present and future of terahertz communications. IEEE Trans. THz Sci. Technol. **1**(1), 256–263 (2011)
[6] Thomas, V.A., Ghafoor, S., El-Hajjar, M., Hanzo, L.: The "Rap" on ROF: radio over fiber using radio access point for high data rate wireless personal area networks. IEEE Microw. Mag. **16**(9), 64–78 (2015)
[7] Xu, K., Wang, R., Dai, Y., Yin, F., Li, J., Ji, Y., Lin, J.: Microwave photonics: radio-over-fiber links, systems, and applications. Photon. Res. **2**(4), B54–B63 (2014)
[8] Al-Raweshidy, H., Komaki, S.: Radio Over Fiber Technologies for Mobile Communications Networks. Artech House, Norwood (2002)
[9] Ho, C.-H., Sambaraju, R., Jiang Jr., W., Lu, T.H., Wang, C.-Y., Yang, H., Lee, W.-Y., Lin, C.-T., Wei, C.-C., Chi, S.: 50-Gb/s radio-over-fiber system employing MIMO and OFDM modulation at 60 GHz. In: Proceedings of Optical Fiber Communications Conference (OFC), Washington, DC, OM2B.3 (2012)
[10] Hsueh, Y.T., Liu, C., Fan, S.H., Yu, J., Chang, G.K.: A novel full-duplex testbed demonstration of converged all-band 60-GHz radio-over-fiber access architecture. In: Proceedings of Optical Fiber Communications Conference (OFC), Washington, DC, OTu2H.5 (2012)
[11] Beltrán, M., Deng, L., Pang, X., Zhang, X., Arlunno, V., Zhao, Y., Yu, X., Llorente, R., Liu, D., Monroy, I. Tafur: 38.2-Gb/s optical-wireless transmission in 75–110 GHz based on electrical OFDM with optical comb expansion. In: Proceedings of Optical Fiber Communications Conference (OFC), Washington, DC, OM2B.2 (2012)
[12] Pleros, N., Vyrsokinos, K., Tsagkaris, K., Tselikas, N.D.: A 60 GHz radio-over-fiber network architecture for seamless communication with high mobility. J. Lightwave Technol. **27**(12), 1957–1967 (2009)
[13] Caballero, A., Zibar, D., Sambaraju, R., Martí, J., Monroy, I.T.: High-capacity 60 GHz and 75–110 GHz band links employing all-optical OFDM generation and digital coherent detection. J. Lightwave Technol. **30**(1), 147–155 (2012)
[14] Shao, T., Beltrán, M., Zhou, R., Anandarajah, P.M., Llorente, R., Barry, L.P.: 60 GHz radio over fiber system based on gain-switched laser. J. Lightwave Technol. **32**(20), 3695–3703 (2014)
[15] Wang, H.M., Hong, W., Chen, J.X., Sun, B., Peng, X.M.: IEEE 802.11 aj (45GHz): a new very high throughput millimeter-wave WLAN system. China Commun. **11**, 51–62 (2014)
[16] Schmuck, H.: Comparison of optical millimetre-wave system concepts with regard to chromatic dispersion. Electron. Lett. **31**(21), 1848–1849 (1995)
[17] Park, J., Sorin, W., Lau, K.: Elimination of the fibre chromatic dispersion penalty on 1550 nm millimetre-wave optical transmission. Electron. Lett. **33**(6), 512–513 (1997)
[18] Smith, G.H., Novak, D., Ahmed, Z.: Overcoming chromatic-dispersion effects in fiber-wireless systems incorporating external modulators. IEEE Trans. Microw. Theory **45**(8), 1410–1415 (1997)
[19] Lorattanasane, C., Kikuchi, K.: Design theory of long-distance optical transmission systems using midway optical phase conjugation. J. Lightwave Technol. **15**(6), 948–955 (1997)
[20] Li, S., Zheng, X., Zhang, H., Zhou, B.: Compensation of dispersion-induced power fading for highly linear radio-over-fiber link using carrier phase-shifted double sideband modulation. Opt. Lett. **36**(4), 546–548 (2011)
[21] Hraimel, B., Zhang, X., Mohamed, M., Wu, K.: Precompensated optical double-sideband subcarrier modulation immune to fiber chromatic-dispersion-induced radio frequency power fading. J. Opt. Commun. Netw. **1**(4), 331–342 (2009)
[22] Zhang, H., Pan, S., Huang, M., Chen, X.: Polarization-modulated analog photonic link with compensation of the dispersion-induced power fading. Opt. Lett. **37**(5), 866–868 (2012)
[23] Pan, S., Yao, J.: A frequency-doubling optoelectronic oscillator using a polarization modulator. IEEE Photon. Technol. Lett. **21**(13), 929–931 (2009)
[24] Yao, X.S., Maleki, L.: Optoelectronic oscillator for photonic systems. IEEE J. Quantum Electron. **32**(7), 1141–1149 (1996)
[25] Pan, S., Yao, J.: Optical clock recovery using a polarization-modulator-based frequency-doubling optoelectronic oscillator. J. Lightwave Technol. **27**(16), 3531–3539 (2009)
[26] Gopalakrishnan, G.K., Burns, W.K., Bulmer, C.H.: Microwave-optical mixing in $LiNbO_3$ modulators. IEEE Trans. Microwave Theory Tech. **41**(12), 2383–2391 (1993)
[27] Bohémond, C., Rampone, T., Sharaiha, A.: Performances of a photonic microwave mixer based on cross-gain modulation in a semiconductor optical amplifier. J. Lightwave Technol. **29**(16), 2402–2409 (2011)
[28] Tang, Z., Zhang, F., Zhu, D., Zou, X., Pan, S.: A photonic frequency downconverter based on a single dual-drive Mach–Zehnder modulator. In: Proceedings of 2013 International Topical Meeting on Microwave Photonics (MWP), pp. 150–153 (2013)
[29] Tang, Z., Zhang, F., Pan, S.: Photonic microwave downconverter based on an optoelectronic oscillator using a single dual-drive Mach–Zehnder modulator. Opt. Express. **22**(1), 305–310 (2014)
[30] Tang, Z., Pan, S.: Distribution of 1.5-Gbps HD video using beamforming-based radio over fiber system. In: Proceedings of Asia Communications and Photonics Conference (ACP), ATh3G.6 (2013)

Zhenzhou Tang received the M.S. degrees in information engineering from Nanjing University of Aeronautics and Astronautics, Nanjing, China, in 2015. He is currently a Ph.D. student in the Key Laboratory of Radar Imaging and Microwave Photonics (Nanjing Univ. Aeronaut. Astronaut.), Ministry of Education. His research interests are radio over fiber systems and microwave photonic mixing.

Shilong Pan received the B.S. and Ph.D. degrees in electronics engineering from Tsinghua University, Beijing, China, in 2004 and 2008, respectively. From 2008 to 2010, he was a "Vision 2010" Postdoctoral Research Fellow in the Microwave Photonics Research Laboratory, University of Ottawa, Canada. He joined the College of Electronic and Information Engineering, Nanjing University of Aeronautics and Astronautics, China, in 2010, where he is currently a full professor and executive director of the Key Laboratory of Radar Imaging and Microwave Photonics (Nanjing Univ. Aeronaut. Astronaut.), Ministry of Education. His research has focused on microwave photonics, which includes optical generation and processing of microwave signals, ultra-wideband over fiber, photonic microwave measurement, and integrated microwave photonics. Prof. Pan has authored or co-authored over 230 research papers, Including more than 110 papers in peer-reviewed journals and 100 papers in conference proceedings. Prof. Pan is a senior member of the IEEE Microwave Theory and Techniques Society, the IEEE Photonics Society and a member of the Optical Society of America. He was selected to receive an OSA outstanding reviewer award in 2015. Prof. Pan is a Chair of numerous international conferences and workshops, including the TPC Chair of the International Conference on Optical Communications and Networks in 2015, TPC Chair of the high-speed and broadband wireless technologies subcommittee of the IEEE Radio Wireless Symposium in 2013, 2014 and 2016, TPC Chair of the Optical fiber sensors and microwave photonics subcommittee chair of the OptoElectronics and Communication Conference in 2015, and Chair of the microwave photonics for broadband measurement workshop of International Microwave Symposium in 2015.